JACS
JOURNAL OF THE AMERICAN CHEMICAL SOCIETY
Communication
pubs.acs.org/JACS

Highly Porous Zirconium Metal–Organic Frameworks with β-UH_3-like Topology Based on Elongated Tetrahedral Linkers

Xin Zhang,[†] Xu Zhang,[†] Jacob A. Johnson,[†] Yu-Sheng Chen,[‡] and Jian Zhang*[,†]

[†]Department of Chemistry, University of Nebraska—Lincoln, Lincoln, Nebraska 68588, United States
[‡]ChemMatCARS, Center for Advanced Radiation Sources, The University of Chicago, 9700 South Cass Avenue, Argonne, Illinois 60439, United States

Supporting Information

ABSTRACT: Two non-interpenetrated zirconium metal–organic frameworks (Zr-MOFs), NPF-200 and NPF-201, were synthesized via the assembly of elongated tetrahedral linkers with Zr_6 and Zr_8 clusters. They represent the first examples of MOFs to have the β-UH_3-like, *4,12,12T1* topology. Upon activation, NPF-200 exhibits the largest BET surface area (5463 m^2 g^{-1}) and void volume (81.6%) among all MOFs formed from tetrahedral ligands. Composed of negative-charged boron-centered tetrahedral linkers, NPF-201 is an anionic Zr-MOF which selectively uptakes photoactive $[Ru(bpy)_3]^{2+}$ for heterogeneous photo-oxidation of thioanisole.

The past two decades have witnessed the rapid development of metal–organic frameworks (MOFs) as a class of highly porous crystalline materials.[1] The tunability of both organic linkers and inorganic metal cluster based secondary building units (SBUs), combined with large surface areas and convenient chemical modification methods, has enabled potential applications of MOFs in areas such as gas storage and separation, catalysis, chemical sensing, and drug delivery, among others.[2] Since many MOFs are water/moisture-sensitive due to the reversible coordination bonding, considerable effort has been focused on MOFs with high thermal and chemical stability for their ultimate practical applications.[3] Zirconium-based MOFs (Zr-MOFs) represent a remarkable improvement to this end:[4] the high valence of Zr^{IV} and large Zr^{IV}–O bond polarization can lead to a strong bonding between Zr^{IV} and carboxylate oxygens in the ligands. Since the discovery of UiO-66 in 2008,[5] Zr-MOFs with rich structural types, outstanding chemical stability, and intriguing properties and functions have made significant progress.[4] Nevertheless, this specific type of MOF is still in its early stage of development. Its wider practical applications call for continuous discovery of new structures with novel topologies, which is important to understanding the fundamental correlation between framework structure and porosity, stability, and interpenetration.[6]

Tetrahedral ligands are inherently three-dimensional, fully extended linkers that have received considerable attention in recent years.[7] However, to date there are only five Zr-MOFs composed of tetrahedral ligands.[8] Four of them, including MOF-841 and PCN-521, have the non-interpenetrated **flu** topology (CaF_2, fluorite),[8] which can be considered as the "pseudo"-*cubic close packing* of the 8-connected Zr_6 clusters, where the octahedral cavity is void space and all the tetrahedral interstitial cavities are occupied by tetrahedral ligands (Figure 1a).[8a] During the synthesis of MOF-841, Yaghi et al. also discovered MOF-812 as a byproduct,[8b] which is essentially a 4,12-connected net of a rare **ith** topology. This topology can be viewed as the *body-centered packing* of 12-connected Zr_6 clusters, where half of the tetrahedral interstitial cavities are occupied by tetrahedral ligands (Figure 1b). Although little study has been performed on MOF-812, its discovery does reveal the possibility for new topologies of Zr-MOFs based on other tetrahedral linkers.

Herein, we report two non-interpenetrated Zr-MOFs, NPF-200 and NPF-201 (where NPF means Nebraska Porous Framework), based on elongated tetrahedral linkers (Figure 1c). Both MOFs belong to the rare *4,12,12T1* topology. Importantly, NPF-200 can be successfully activated and exhibits 81.6% solvent-accessible volume and a BET surface area of 5463 m^2 g^{-1}, which is the largest among the MOFs formed from tetrahedral ligands and also the third largest among all Zr-MOFs. Additionally, the isostructural NPF-201, featuring a tetravalent boron-centered linker, is an anionic Zr-MOF that selectively uptakes $[Ru(bpy)_3]^{2+}$.

The two tetrahedral linkers, $\mathbf{L}_4$ and $\mathbf{L}_5$, were synthesized by Sonogashira coupling, followed by saponification in basic aqueous solution (see Supporting Information (SI), section S-3, for detailed procedures). Colorless crystals of NPF-200 $[Zr_6(\mu_3\text{-}O)_4(\mu_3\text{-}OH)_4]_3[Zr_8(\mu_2\text{-}O(H))_{12}](\mathbf{L}_4)_{12}$ were obtained via a solvothermal reaction of $ZrCl_4$ with $\mathbf{L}_4$ in *N*,*N*-dimethylformamide (DMF) with benzoic acid as modulating agent[9] at 120 °C for 48 h. Single-crystal X-ray diffraction reveals that NPF-200 crystallizes in the cubic space group $Pm\bar{3}n$, consistent with the truncated octahedral shape of the single crystals (SI, Figure S7). The experimental powder X-ray diffraction (PXRD) patterns of NPF-200 are in excellent agreement with the simulation (Figure 2a), demonstrating the material's bulk purity.

NPF-200 is a non-interpenetrated framework that is composed of two different types of 12-connected Zr clusters (Zr_6 and Zr_8) linked by tetrahedral ligands (Figure 1c). Overall, it is a trinodal net with the 4,12,12T1 topology with point symbol $(4^{28}.6^{32}.8^6)_3(4^{30}.6^{30}.8^6)(4^6)_{12}$ which is the same observed for that of β-UH_3.[10] It is noteworthy that NPF-200 represents the first MOF structure that exhibits this rare topology. The Zr_6 and Zr_8 clusters in NPF-200 can be envisioned as the topological close

Received: May 4, 2016
Published: June 24, 2016

DOI: 10.1021/jacs.6b04608
J. Am. Chem. Soc. 2016, 138, 8380–8383

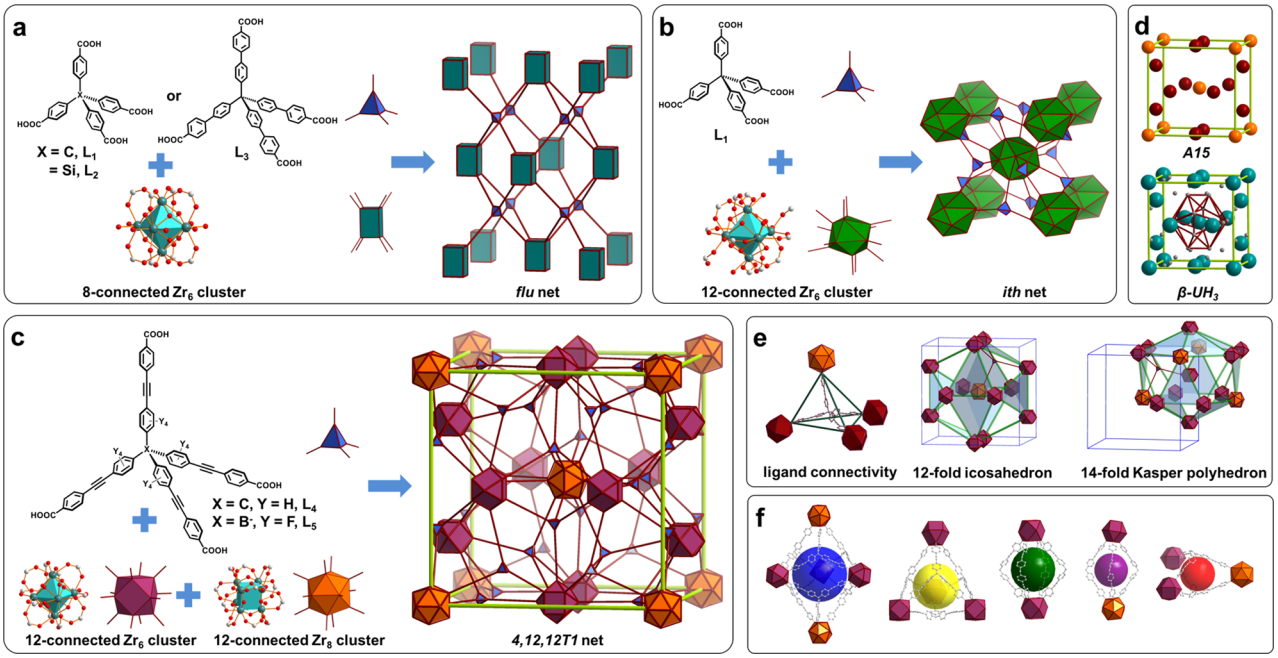

Figure 1. Tetrahedral linkers and Zr clusters, their topological representations (C, gray; O, red; Zr, cyan), and augmented topology of (a) PCN-521 and MOF-841 (**flu** topology), (b) MOF-812 (**ith** topology), and (c) NPF-200 and 201 (*4,12,12T1* topology). The blue, cyan, purple, and gold polyhedra represent 4-, 8-(Zr_6), 12-(Zr_6), and 12-(Zr_8)-connected nodes, respectively. (d) Frank–Kasper A15 phase and crystal structure of β-UH_3. (e) The connectivity of the tetrahedral linker, Zr_6, and Zr_8 cluster. (f) Five different pore structures featured in NPF-200 and 201.

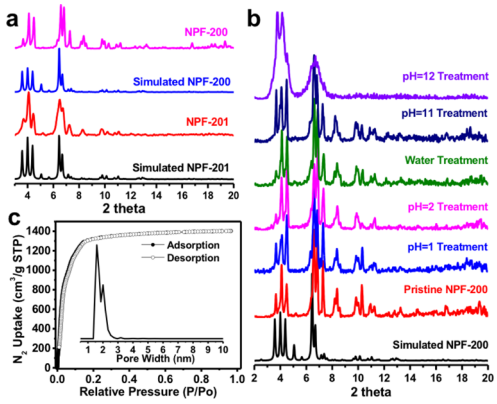

Figure 2. (a) PXRD of NPF-200 and NPF-201. (b) PXRD of NPF-200 after treatment at acidic and basic conditions. (c) N_2 adsorption isotherms and pore size distribution of NPF-200.

packing phase A15 (Figure 1d),[11] one of the Frank–Kasper phases used to describe the structures of intermetallics with A_3B stoichiometry (e.g., Nb_3Sn)[12] and certain self-assembled macromolecules.[13] In a typical cubic unit cell, B atoms (as Zr_8 clusters in NPF-200) occupy the *body-centered cubic* sites while a pair of A atoms (as Zr_6 clusters in NPF-200) occupy the *face-centered* sites, furthering linking in infinite chains along the [100], [010], and [001] directions. Therefore, Zr_8 clusters in NPF-200 lie in the center of the 12-fold distorted icosahedron (as B atoms in A15), and Zr_6 clusters lie in the center of a 14-fold Kasper polyhedron (as A atoms in A15) (Figure 1e). Each tetrahedral ligand is connected with three Zr_6 clusters and one Zr_8 cluster (Figure 1e), just like the H-atoms in β-UH_3. (Figure 1d). Since the A15 phase has exclusively tetrahedral interstices (see SI, section S-7, for detailed description), NPF-200 can also be considered, as part of its tetrahedral interstitial cavities are occupied by tetrahedral ligands (Figure 1e). On average, 24 tetrahedral ligands occupy 46 interstitial tetrahedra in each unit cell, giving rise to a 52.2% occupancy compared to 50% in MOF-812. Further, five well-defined cages with sizes ranging from 12 to 20 Å can be identified in NPF-200 (Figure 1f and SI, Figures S15–S19).

The Zr_6 cluster in NPF-200 is the commonly observed, 12-connected $Zr_6(\mu_3\text{-O})_4(\mu\text{-OH})_4$ in many Zr-MOFs (i.e., UiO-66 and its isoreticular *fcu* series[5]), which can be simplified as a cuboctahedron (SI, Figure S20). In contrast, the Zr_8 cluster in NPF-200 is best described as $Zr_8(\mu_2\text{-O(H)})_{12}$, with eight Zr atoms connecting 12 μ_2-O(H), forming a cubic Zr cluster in which the eight vertices are occupied by Zr atoms capped by 12 μ_2-O(H) occupying the edges (Figure 1c; see SI, section S-2, for details). The simplified Zr_8 cluster in NPF-200 corresponds to a slightly distorted icosahedron (SI, Figure S21), which nevertheless is more regular compared to that of the Zr_6 clusters in MOF-812 (SI, Figure S20), likely due to the coordination of four monodentate carboxylate groups in the latter. In NPF-200, each Zr atom in the Zr_8 cluster coordinates with three μ_2-O(H) and three oxygen atoms from carboxylates, forming a distorted octahedral coordination geometry. Compared to the Zr_6 cluster, the Zr_8 cluster is much less common. Zhou et al. previously reported an example of cubic Zr_8 cluster, $Zr_8(\mu_4\text{-O})_6(OH)_8$, in PCN-221, where each edge of the Zr_8 cube is bridged by a carboxylate group, and the simplified SBU corresponds to a cuboctahedron with O_h symmetry (SI, Figure S21).[14] Our result represents the second example of Zr_8 cluster in Zr-MOF.

The thermal stability of NPF-200 was assessed by thermogravimetric analysis. The high decomposition temperature around 450 °C reveals the excellent thermal stability of the material at elevated temperature (SI, Figure S25). NPF-200 shows remarkable stability in acidic and basic conditions (Figure 2b). After soaking in aqueous solutions with pH values ranging from 1 to 11 (prepared with HCl and NaOH respectively) for 24 h, the PXRD patterns of NPF-200 are almost unchanged, suggesting the preserved crystallinity (Figure 2b). The N_2

DOI: 10.1021/jacs.6b04608
J. Am. Chem. Soc. 2016, 138, 8380–8383

adsorption of NPF-200 after water treatment (SI, Figure S11) exhibits only a minimal deviation from that of the pristine sample, indicating the framework is highly robust. However, NPF-200 does start to lose crystallinity after being soaked in a strongly basic solution (pH 12) (Figure 2b).

Supercritical CO_2 exchange[15] was employed to activate NPF-200 to avoid channel collapse. With a pore volume of 2.17 $cm^3\ g^{-1}$, NPF-200 has N_2 uptake at 77 K of 1403 $cm^3\ g^{-1}$, SA_{BET} (Brunauer–Emmett–Teller surface area) of 5463 $m^2\ g^{-1}$, and $SA_{Langmuir}$ (Langmuir surface area) of 6877 $m^2\ g^{-1}$. Based on the calculated value by PLATON, the solvent-accessible volume is 81.6%.[16] It is noted that NPF-200 has the largest surface area, pore size, and solvent-accessible volume among all MOFs constructed from tetrahedral ligands. The calculated volumetric surface area of NPF-200 is 2125 $m^2\ cm^{-3}$, which is outstanding among many well-known MOFs (SI, Table S3). For certain gas uptake applications, a large volumetric surface area is crucial.[17]

Isoreticular expansion[18] is a useful strategy to increase the pore size and surface area for Zr-MOFs.[19] It is, however, interesting to note that the ligand elongation in NPF-200 did not result in the expected **flu** topology as in PCN-521. The increased rotational freedom from $\mathbf{L}_3$ (in PCN-521) to $\mathbf{L}_4$ (in NPF-200) likely plays a role here. In order to fulfill the coordination and topological requirement in NPF-200 (i.e., binding with one Zr_8 and three Zr_6 clusters in *4,12,12T1* topology), the tetrahedral ligand $\mathbf{L}_4$ needs to adopt a C_{2v} symmetry so that the two peripheral benzoates are perpendicularly orientated to one pseudo-mirror plane and two peripheral benzoates lying in the other (Figure 3a). Such

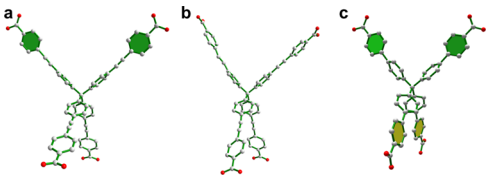

Figure 3. Conformation of peripheral benzoates in (a) $\mathbf{L}_4$ in NPF-200 (two peripheral benzoates lying in one mirror plane), (b) $\mathbf{L}_4$ in MOF $Cu_2\mathbf{L}_4$, and (c) $\mathbf{L}_3$ in PCN-521 (four peripheral benzoates lying in two mirror planes). Green and yellow colors highlight the benzoate rings lying in the mirror planes.

conformation is made possible by the triple-bond spacer between the two phenyl rings that promotes low to no torsional barrier for the vicinal phenyl rings.[20] Indeed, other conformations of $\mathbf{L}_4$ are possible, as exemplified in MOF $Cu_2\mathbf{L}_4$ reported by Lin et al., where all four peripheral benzoates are perpendicularly orientated to the mirror planes (Figure 3b).[7f] Conversely, in PCN-521, all four peripheral benzoates of $\mathbf{L}_3$, which has D_{2d} symmetry, lie in the two mirror planes to meet the requirement of coordination to four Zr_6 clusters in the **flu** topology (Figure 3c). Further, in the absence of spacer, the reduced rotational freedom between the two phenyl rings in $\mathbf{L}_3$ makes it unfavorable to adopt a zero dihedral angle, which is required to adopt a conformation similar to that of $\mathbf{L}_4$ to form the *4,12,12T1* topology.

The success in synthesizing NPF-200 offers a general way of constructing non-interpenetrated Zr-MOFs with exceptional high porosity. We next set out to synthesize an isostructure of NPF-200 using a boron-centered tetrahedral linker $\mathbf{L}_5$ (Figure 1d; see SI, section S-2, for synthetic details) that has essentially the same size and dimensionality as $\mathbf{L}_4$. Since $\mathbf{L}_5$ is inherently negatively charged, the resulting MOF is expected to be an anionic Zr-MOF. Both single-crystal XRD (SI, section S-4) and the PXRD pattern (Figure 2a) show that the product from the solvothermal reaction of $ZrCl_4$ and $\mathbf{L}_5$, called NPF-201, is isostructural with NPF-200. However, activation of NPF-201 was not successful, and SA_{BET} of NPF-201 was only 534 $m^2\ g^{-1}$, probably due to the framework collapse induced by the extraframework countercation, tetrabutylammonium. Nevertheless, NPF-201 still exhibits good thermal stability (thermal decomposition temperature of 400 °C, SI, Figure S26) and chemical stability in solution (SI, Figure S10), which enable its potential applications in the solvated state, including heterogeneous catalysis.

The anionic charge of the framework of NPF-201 was further confirmed by dye exchange experiments. As expected, NPF-201 does not adsorb the anionic dye, acid orange 7, but strongly adsorbs the cationic methylene blue (Figure 4a). The adsorbed

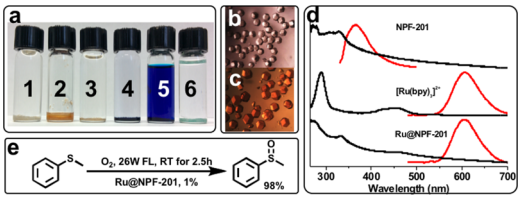

Figure 4. (a) Selective ion exchange of NPF-201: as prepared (1), after soaking in acid orange 7 for 24 h (2), after subsequent washing with DMF (3), after soaking in methylene blue for 24 h and subsequent washing with DMF (4), and after further soaking in 0.5 M NH_4Cl solution (5) and washing with DMF (6). Photographs of single crystals of NPF-201 before (b) and after (c) uptake of $[Ru(bpy)_3]^{2+}$. (d) UV–vis (black) and fluorescence (red) spectra of NPF-201, $[Ru(bpy)_3]^{2+}$, and Ru@NPF-201. (e) Photocatalytic oxidation of thioanisole.

methylene blue can be further exchanged by soaking in 0.5 M NH_4Cl solution (Figure 4a). To the best of our knowledge, NPF-201 represents the first example of anionic Zr-MOF.[21] This feature opens enormous opportunities to incorporate functional cationic guests into Zr-MOFs for a variety of applications.[22] Here, a photoactive cationic transition metal complex, $[Ru(bpy)_3]^{2+}$, was incorporated into NPF-201 via ion exchange to form Ru@NPF-201 (Figure 4b,c). The loading level of $[Ru(bpy)_3]^{2+}$, 0.37 Ru complex per ligand, was determined using NMR spectroscopy of an acid-digested sample (SI, Figure S8). This loading value is close to the ideal uptake (0.5 per ligand), suggesting the successful incorporation of the metal complex inside the framework. Ru@NPF-201 exhibits the characteristic emission band of $[Ru(bpy)_3]^{2+}$ at 600 nm (Figure 4d) and can be used as a heterogeneous catalyst in photooxidation of thioanisole. Indeed, while NPF-201 does not show any activity at all, Ru@NPF-201 gives rise to the sulfoxide product in an excellent yield (98%), with a catalytic activity comparable to that of $[Ru(bpy)_3]^{2+}$, indicating that the reaction is not diffusion limited (SI, section S-9 and Table S2). Importantly, Ru@NPF-201 exhibits excellent recyclability: after five times of reuse, no decrease of catalytic activity is observed (SI, Table S2).

In summary, we have synthesized two new non-interpenetrated Zr-MOFs with the rare β-UH_3-like, *4,12,12T1* topology using elongated tetrahedral linkers. NPF-200 exhibits high permanent porosity (2.17 $cm^3\ g^{-1}$), large surface area (5463 $m^2\ g^{-1}$), and exceptional stability, which make it a promising candidate material for gas storage. Anionic NPF-201 successfully incorporates photoactive $[Ru(bpy)_3]^{2+}$ via cation exchange, and the resulting hybrid material exhibits good photocatalytic activity

DOI: 10.1021/jacs.6b04608
J. Am. Chem. Soc. 2016, 138, 8380–8383

and recyclability toward the photo-oxidation of thioanisole. Our work points to a new direction for designing functional Zr-MOFs with new topologies using elongated tetrahedral linkers.

■ ASSOCIATED CONTENT

Supporting Information

The Supporting Information is available free of charge on the ACS Publications website at DOI: 10.1021/jacs.6b04608.

Materials, general experimental procedures, synthesis of NPF-200 and NPF-201, characterizations of compounds, topology analysis, photocatalytic studies, and crystallographic data (PDF)

X-ray crystallographic data for NPF-200 (CIF)

X-ray crystallographic data for NPF-201 (CIF)

■ AUTHOR INFORMATION

Corresponding Author

*jzhang3@unl.edu

Notes

The authors declare no competing financial interest.

■ ACKNOWLEDGMENTS

We thank Prof. Davide M. Proserpio for assistance with topology analysis and Profs. Oleh Khalimonchuk and Donald Becker for help with UV−vis measurements of MOFs. The authors acknowledge the support from the University of Nebraska−Lincoln. ChemMatCARS Sector 15 is principally supported by the Divisions of Chemistry (CHE) and Materials Research (DMR), National Science Foundation, under grant no. NSF/CHE-1346572. Use of the APS, an Office of Science User Facility operated for the U.S. DOE Office of Science by ANL, was supported under Contract No. DE-AC02-06CH11357.

■ REFERENCES

(1) (a) Zhou, H. C.; Long, J. R.; Yaghi, O. M. *Chem. Rev.* **2012**, *112*, 673−674. (b) Furukawa, H.; Cordova, K. E.; O'Keeffe, M.; Yaghi, O. M. *Science* **2013**, *341*, 1230444. (c) Cook, T. R.; Zheng, Y. R.; Stang, P. J. *Chem. Rev.* **2013**, *113*, 734−777. (d) Zhou, H. C.; Kitagawa, S. *Chem. Soc. Rev.* **2014**, *43*, 5415−5418.

(2) (a) Suh, M. P.; Park, H. J.; Prasad, T. K.; Lim, D. W. *Chem. Rev.* **2012**, *112*, 782−835. (b) Kreno, L. E.; Leong, K.; Farha, O. K.; Allendorf, M.; Van Duyne, R. P.; Hupp, J. T. *Chem. Rev.* **2012**, *112*, 1105−1125. (c) He, Y.; Zhou, W.; Qian, G.; Chen, B. *Chem. Soc. Rev.* **2014**, *43*, 5657−5678. (d) Hu, Z.; Deibert, B. J.; Li, J. *Chem. Soc. Rev.* **2014**, *43*, 5815−5840. (e) Zhang, T.; Lin, W. *Chem. Soc. Rev.* **2014**, *43*, 5982−5993. (f) Sun, L.; Campbell, M. G.; Dincă, M. *Angew. Chem., Int. Ed.* **2016**, *55*, 3566−3579. (g) Dhakshinamoorthy, A.; Asiri, A. M.; García, H. *Angew. Chem., Int. Ed.* **2016**, *55*, 5414−5445.

(3) (a) Férey, G.; Mellot-Draznieks, C.; Serre, C.; Millange, F.; Dutour, J.; Surblé, S.; Margiolaki, I. *Science* **2005**, *309*, 2040−2042. (b) Nguyen, J. G.; Cohen, S. M. *J. Am. Chem. Soc.* **2010**, *132*, 4560−4561. (c) Decoste, J. B.; Peterson, G. W.; Smith, M. W.; Stone, C. A.; Willis, C. R. *J. Am. Chem. Soc.* **2012**, *134*, 1486−1489. (d) Devic, T.; Serre, C. *Chem. Soc. Rev.* **2014**, *43*, 6097−6115. (e) Burtch, N. C.; Jasuja, H.; Walton, K. S. *Chem. Rev.* **2014**, *114*, 10575−10612.

(4) Bai, Y.; Dou, Y.; Xie, L. H.; Rutledge, W.; Li, J. R.; Zhou, H. C. *Chem. Soc. Rev.* **2016**, *45*, 2327−2367.

(5) Cavka, J. H.; Jakobsen, S.; Olsbye, U.; Guillou, N.; Lamberti, C.; Bordiga, S.; Lillerud, K. P. *J. Am. Chem. Soc.* **2008**, *130*, 13850−13851.

(6) (a) Blatov, V. A.; Carlucci, L.; Ciani, G.; Proserpio, D. M. *CrystEngComm* **2004**, *6*, 378−395. (b) Li, M.; Li, D.; O'Keeffe, M.; Yaghi, O. M. *Chem. Rev.* **2014**, *114*, 1343−1370.

(7) (a) Chen, B.; Eddaoudi, M.; Reineke, T. M.; Kampf, J. W.; O'Keeffe, M.; Yaghi, O. M. *J. Am. Chem. Soc.* **2000**, *122*, 11559−11560. (b) Kim, J.; Chen, B.; Reineke, T. M.; Li, H.; Eddaoudi, M.; Moler, D. B.; O'Keeffe, M.; Yaghi, O. M. *J. Am. Chem. Soc.* **2001**, *123*, 8239−8247. (c) Chun, H.; Kim, D.; Dybtsev, D. N.; Kim, K. *Angew. Chem., Int. Ed.* **2004**, *43*, 971−974. (d) Cheon, Y. E.; Suh, M. P. *Chem. Commun.* **2009**, 2296−2298. (e) Ma, L.; Jin, A.; Xie, Z.; Lin, W. *Angew. Chem., Int. Ed.* **2009**, *48*, 9905−9908. (f) Liu, D.; Xie, Z.; Ma, L.; Lin, W. *Inorg. Chem.* **2010**, *49*, 9107−9109. (g) Zhang, M.; Chen, Y.-P.; Zhou, H.-C. *CrystEngComm* **2013**, *15*, 9544.

(8) (a) Zhang, M.; Chen, Y. P.; Bosch, M.; Gentle, T., III; Wang, K.; Feng, D.; Wang, Z. U.; Zhou, H. C. *Angew. Chem., Int. Ed.* **2014**, *53*, 815−818. (b) Furukawa, H.; Gándara, F.; Zhang, Y. B.; Jiang, J.; Queen, W. L.; Hudson, M. R.; Yaghi, O. M. *J. Am. Chem. Soc.* **2014**, *136*, 4369−4381. (c) Wang, S.; Wang, J.; Cheng, W.; Yang, X.; Zhang, Z.; Xu, Y.; Liu, H.; Wu, Y.; Fang, M. *Dalton Trans.* **2015**, *44*, 8049−8061. (d) Ma, J.; Tran, L. D.; Matzger, A. J. *Cryst. Growth Des.* **2016**, DOI: 10.1021/acs.cgd.6b00698.

(9) Schaate, A.; Roy, P.; Godt, A.; Lippke, J.; Waltz, F.; Wiebcke, M.; Behrens, P. *Chem. - Eur. J.* **2011**, *17*, 6643−6651.

(10) (a) Rundle, R. E. *J. Am. Chem. Soc.* **1951**, *73*, 4172−4174. (b) Taylor, C. D. *Phys. Rev. B: Condens. Matter Mater. Phys.* **2010**, *82*, 224408. (c) Blatov, V. A.; Shevchenko, A. P.; Proserpio, D. M. *Cryst. Growth Des.* **2014**, *14*, 3576−3586.

(11) Graef, M. D.; Mchenry, M. E. *Structure of Materials: An Introduction to Crystallography, Diffraction and Symmetry*, 2nd ed.; Cambridge Univ. Press: Cambridge, UK, 2012.

(12) Frank, F. C.; Kasper, J. S. *Acta Crystallogr.* **1958**, *11*, 184−190.

(13) Huang, M.; Hsu, C. H.; Wang, J.; Mei, S.; Dong, X.; Li, Y.; Li, M.; Liu, H.; Zhang, W.; Aida, T.; Zhang, W. B.; Yue, K.; Cheng, S. Z. *Science* **2015**, *348*, 424−428.

(14) Feng, D.; Jiang, H. L.; Chen, Y. P.; Gu, Z. Y.; Wei, Z.; Zhou, H. C. *Inorg. Chem.* **2013**, *52*, 12661−12667.

(15) Nelson, A. P.; Farha, O. K.; Mulfort, K. L.; Hupp, J. T. *J. Am. Chem. Soc.* **2009**, *131*, 458−460.

(16) Spek, A. L. *J. Appl. Crystallogr.* **2003**, *36*, 7−13.

(17) Spanopoulos, I.; Tsangarakis, C.; Klontzas, E.; Tylianakis, E.; Froudakis, G.; Adil, K.; Belmabkhout, Y.; Eddaoudi, M.; Trikalitis, P. N. *J. Am. Chem. Soc.* **2016**, *138*, 1568−1574.

(18) (a) Yaghi, O. M.; O'Keeffe, M.; Ockwig, N. W.; Chae, H. K.; Eddaoudi, M.; Kim, J. *Nature* **2003**, *423*, 705−714. (b) Furukawa, H.; Ko, N.; Go, Y. B.; Aratani, N.; Choi, S. B.; Choi, E.; Yazaydin, A. Ö.; Snurr, R. Q.; O'Keeffe, M.; Kim, J.; Yaghi, O. M. *Science* **2010**, *329*, 424−428. (c) Farha, O. K.; Yazaydin, A. Ö.; Eryazici, I.; Malliakas, C. D.; Hauser, B. G.; Kanatzidis, M. G.; Nguyen, S. T.; Snurr, R. Q.; Hupp, J. T. *Nat. Chem.* **2010**, *2*, 944−948. (d) Farha, O. K.; Eryazici, I.; Jeong, N. C.; Hauser, B. G.; Wilmer, C. E.; Sarjeant, A. A.; Snurr, R. Q.; Nguyen, S. T.; Yazaydin, A. Ö.; Hupp, J. T. *J. Am. Chem. Soc.* **2012**, *134*, 15016−15021.

(19) (a) Wang, T. C.; Bury, W.; Gómez-Gualdrón, D. A.; Vermeulen, N. A.; Mondloch, J. E.; Deria, P.; Zhang, K.; Moghadam, P. Z.; Sarjeant, A. A.; Snurr, R. Q.; Stoddart, J. F.; Hupp, J. T.; Farha, O. K. *J. Am. Chem. Soc.* **2015**, *137*, 3585−3591. (b) Liu, T. F.; Feng, D.; Chen, Y. P.; Zou, L.; Bosch, M.; Yuan, S.; Wei, Z.; Fordham, S.; Wang, K.; Zhou, H. C. *J. Am. Chem. Soc.* **2015**, *137*, 413−419.

(20) Okuyama, K.; Hasegawa, T.; Ito, M.; Mikami, N. *J. Phys. Chem.* **1984**, *88*, 1711−1716.

(21) Zhang, Q.; Yu, J.; Cai, J.; Zhang, L.; Cui, Y.; Yang, Y.; Chen, B.; Qian, G. *Chem. Commun.* **2015**, *51*, 14732−14734.

(22) (a) An, J.; Geib, S. J.; Rosi, N. L. *J. Am. Chem. Soc.* **2009**, *131*, 8376−8377. (b) Sun, C. Y.; Wang, X. L.; Zhang, X.; Qin, C.; Li, P.; Su, Z. M.; Zhu, D. X.; Shan, G. G.; Shao, K. Z.; Wu, H.; Li, J. *Nat. Commun.* **2013**, *4*, 2717. (c) Yu, J.; Cui, Y.; Xu, H.; Yang, Y.; Wang, Z.; Chen, B.; Qian, G. *Nat. Commun.* **2013**, *4*, 2719. (d) Zhao, X.; Bu, X.; Wu, T.; Zheng, S. T.; Wang, L.; Feng, P. *Nat. Commun.* **2013**, *4*, 2344. (e) Johnson, J. A.; Zhang, X.; Zhang, X.; Zhang, J. *Curr. Org. Chem.* **2014**, *18*, 1973−2001. (f) Aubrey, M. L.; Long, J. R. *J. Am. Chem. Soc.* **2015**, *137*, 13594−13602. (g) Wang, X.; Lu, W.; Gu, Z. Y.; Wei, Z.; Zhou, H. C. *Chem. Commun.* **2016**, *52*, 1926−1929.